Journal of Inflammation Research

Dovepress
open access to scientific and medical research

Open Access Full Text Article

ORIGINAL RESEARCH

Suppression of CGRP and TRPV1 Expression in Dorsal Root Ganglia of Knee Osteoarthritis Rats by Huojing Decoction via TrkA/MKK3/6/p38 Pathway

Xinchao Jiang[1,*], Yinyin Guo[2,*], Mei Fang[1], Xin Wang[3], Biao Zhang[4], Yi Song[1], Jianxue Qian[1]

[1]Department of Pain Medicine, Suzhou Hospital of Integrated Traditional Chinese and Western Medicine, Suzhou, Jiangsu, People's Republic of China; [2]Department of Oncology, Suzhou Hospital of Integrated Traditional Chinese and Western Medicine, Suzhou, Jiangsu, People's Republic of China; [3]Department of Nephrology, Suzhou Hospital of Integrated Traditional Chinese and Western Medicine, Suzhou, Jiangsu, People's Republic of China; [4]Department of Intensive Care, Suzhou Hospital of Integrated Traditional Chinese and Western Medicine, Suzhou, Jiangsu, People's Republic of China

*These authors contributed equally to this work

Correspondence: Jianxue Qian; Yi Song, Department of Pain Medicine, Suzhou Hospital of Integrated Traditional Chinese and Western Medicine, 39 Xiashatang Road, Wuzhong District, Suzhou, Jiangsu, People's Republic of China, Tel/Fax +86 0512-69388313; +86 0512-69388412, Email szxqjx@126.com; 376063583@qq.com

Objective: Knee osteoarthritis (KOA) is a chronic condition characterized by persistent pain that can lead to severe disability. In this study, we primarily investigated the analgesic effect of Huojing decoction on MIA-induced knee arthritis.

Methods: The network pharmacology method was employed to acquire target information of Huojing decoction and KOA. MIA was intratibially injected to induce KOA pain in rats. Huojing decoction was then administered once daily via intragastric administration for 14 days. Pain level was assessed by paw withdrawal threshold (PWT) and paw withdrawal latency (PWL). The levels of inflammatory cytokines were determined by ELISA and PCR. TRPV1 and CGRP were detected through immunohistochemistry. The protein expression of TrkA, MKK3/6 and p38 was assessed by Western blot.

Results: Mechanical allodynia and thermal hyperalgesia were observed in KOA rats. The expression levels of inflammatory cytokines were significantly decreased after Huojing decoction infusion of KOA rats. TRPV1 and CGRP were reduced with treatment. Furthermore, the protein expressions of TrkA, MKK3/6 and p38 in the DRG of rats were significantly decreased.

Conclusion: Our data suggested that Huojing decoction can alleviate inflammation in KOA pain rats. Additionally, it can inhibit the expression of TrKA, MKK3/6 and p38 signaling pathways, indicating its analgesic effect on KOA pain rats.

Keywords: huojing decoction, analgesic effect, knee osteoarthritis, dorsal root ganglion, TrkA/MKK3/6/p38 pathway

Introduction

Osteoarthritis (OA) is a common chronic joint disease that often affects middle-aged and elderly individuals. It typically manifests in joints subjected to frequent use, heavy burden, and high activity, including knee, hip, spine, ankle and others.[1] Among the different types of OA, knee osteoarthritis (KOA) is particularly widespread. According to the latest epidemiological survey in China. Currently, the prevalence rate of symptomatic knee osteoarthritis (KOA) is 8.1%. This implies that approximately 110 million people across the country have KOA. Notably, the prevalence of KOA among individuals over 65 years old has reached 50%.[2] The disabling effects of knee osteoarthritis are often accompanied by alterations in joint biomechanics and the development of induced and spontaneous pain associated with arthritis. In severe cases, these factors can lead to joint disability and adversely impact the quality of life for affected patients.[3]

KOA pain is mainly considered as inflammatory pain. Chondrocytes and synovial tissues have the capacity to produce interleukin (IL) and Tumor necrosis factor (TNF), among other inflammatory factors. These factors can disrupt the structure and function of synovial tissue and chondrocytes, promoting their apoptosis. Eventually, it results in the degradation of

Received: 2 June 2024
Accepted: 3 August 2024
Published: 13 August 2024

Graphical Abstract

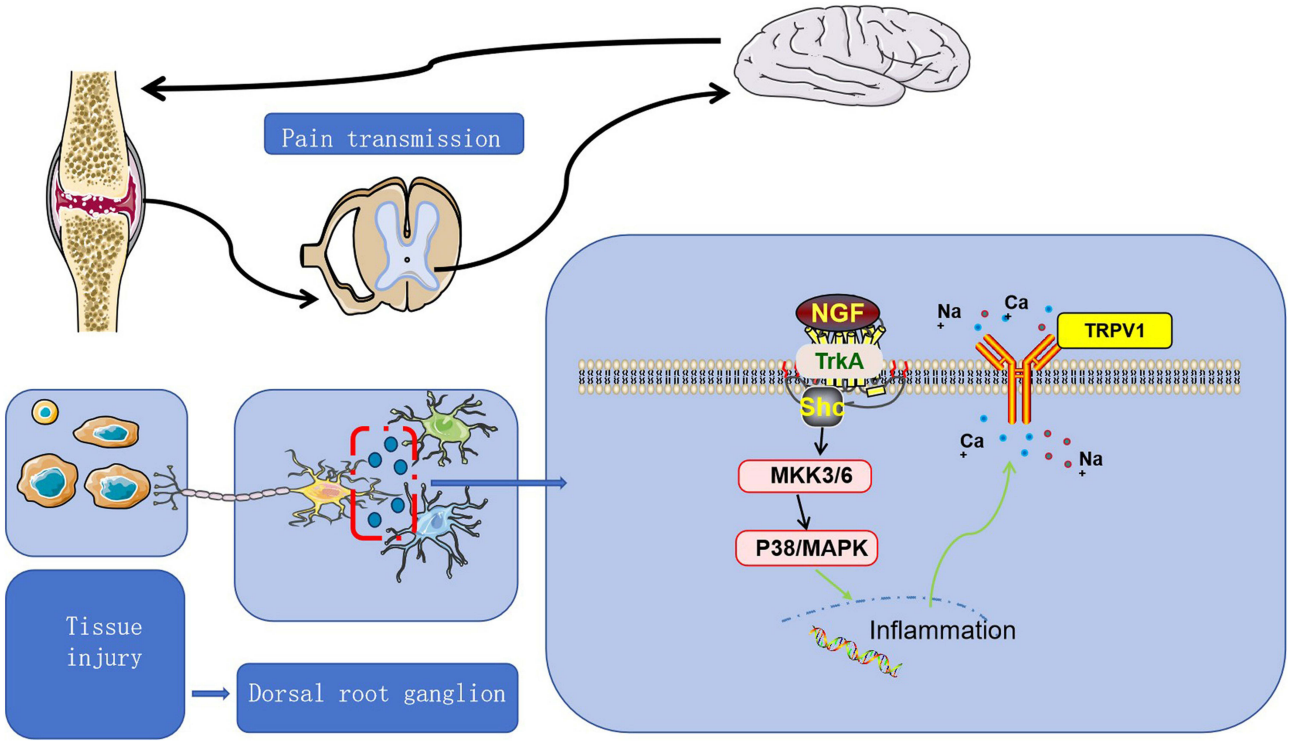

articular cartilage extracellular matrix and the sclerosis of subchondral bone.[4,5] Various inflammatory factors contribute to the pain in KOA, among which IL and TNF are the most prominent, such as IL-1β, IL-6, and TNF-α.[6,7] Inflammation plays an important role in maintaining the balance of the knee joint's new aging and internal environment. IL-1β not only induces inflammation but also cooperates with other inflammatory factors to magnify the inflammatory response. Eventually, it facilitates the degradation of cartilage.[8] As the disease progress, sustained inflammatory stimulation and ongoing neuron damage may lead to pain sensitization and the loss of peripheral nerve fibers. This process further induces overactivity of spinal dorsal root ganglion (DRG) neurons, ultimately resulting in central sensitization and heightened pain sensitivity.[9]

Huojing decoction (HJD) is comprised of *Saposhnikovia divaricata (Turcz. ex Ledeb). Schischk, Neolitsea cassia (L). Kosterm, Hansenia weberbaueriana (Fedde ex H.Wolff) Pimenov & Kljuykov, Angelica biserrata (R.H.Shan & C.Q.Yuan) C.Q.Yuan & R.H.Shan, Gentiana macrophylla Pall, Atractylodes lancea (Thunb). DC, Atractylodes macrocephala Koidz, Arisaema erubescens (Wall). Schott* and *Pinellia ternata (Thunb). Makino*. Known for its ability to dispel wind and dampness and alleviate pain, our present data surprisingly demonstrated that HJD could relieve hyperalgesia in KOA rats and downregulate the expression levels of IL-1β, IL-6 and TNF-α in DRG.

The p38 mitogen-activated protein kinase (p38) is a member of the MAPK family and plays a critical role in inflammation and neuropathic pain. Understanding its mechanisms of involvement can help elucidate the process of pain occurrence and potentially identify new targets for pain treatment.[10] A previous research indicated that the activation of the p38 pathway triggered the release of inflammatory cytokines.[11] Monoiodoacetic acid (MIA) was found to promote the phosphorylation of p38. This promoting effect was the most significant after the injection of MIA. This led to an increased expression of ipsilateral microglia. And it caused central sensitization in the MIA-induced osteoarthritis (MIA-OA) experimental pain model.[12] Recent evidence suggests that inhibiting the p38 signaling pathways contributes to the downregulation of IL-1β, IL-6, and TNF-α expression. This reduction is capable of alleviating mechanical sensitivity and thermal hypersensitivity, improving neuroinflammation and reducing neuropathic pain.[13,14]

On the other hand, it has been proven that the pain is closely associated with transient receptor potential vanilloid 1 (TRPV1) and calcitonin gene-related peptide (CGRP). MIA administration, inducing OA has been shown to increase the expression of CGRP and TRPV1.[15,16] The progression of OA can readily trigger the activation and overexpression of TRPV1. Downregulating TRPV1 expression might alleviate chronic inflammatory pain, providing potential therapeutic targets for osteoarthritis patients.[17] Furthermore, the activation of TRPV1 and release of CGRP were identified in the DRG of a mouse pain model. Inhibiting TRPV1 activation and CGRP release could improve mechanical hyperalgesia, thermal hyperalgesia and weight distribution issues.[18]

In our preliminary experiments, it was found that HJD has effective analgesic and anti-inflammatory effects on MIA-induced KOA rats. However, the potential functional mechanism remains to be investigated. Therefore, we plan to construct a MIA-induced KOA rat model for in vivo experiments and use HJD treatment to intervene in the rats' treatment. We aim to explore whether Huojing treatment can alleviate pain hypersensitivity by suppressing CGRP and TRPV1 expression through TrkA/MKK3/6/p38 pathway.

Materials and Methods

Network Pharmacology Research and Ethical Statement

This research strictly adheres to international and domestic ethical guidelines and legal regulations governing the use of human data. The research protocol was thoroughly reviewed and approved by the Suzhou Hospital of Integrated Chinese and Western Medicine's ethics committee (Approval Number:2024008). We utilized the TCMSP database to search for HJD components and targets. Additionally, we explored the GeneCards database and the OMIM database using the keyword "knee arthritis". The screened HJD active ingredient targets and KOA targets were inputted into the Venn diagram making software Venny 2.1 to identify the common targets. These common targets were then inputted into the String database to construct the Protein-Protein Interaction (PPI) network. The PPI network was imported into Cytoscape for analysis. Subsequently, common targets of HJD and KOA underwent GO enrichment analysis and KEGG pathway enrichment analysis. This process aimed to identify the key active ingredients and targets of HJD.

UPLC-MS/MS of HJD

LCMS-8050 ultra-high performance liquid chromatography-mass spectrometer (Shimadzu, Japan) was used in the detection. The Ultra-high performance liquid chromatography-tandem mass spectrometry (UPLC-MS/MS) method and negative ion multiple reaction monitoring (MRM) mode were used for content determination. The chromatographic column was Waters CORTECS C18 (2.1 mm × 100 mm, 1.6 μm), the mobile phase was acetonitrile (A) − 0.1% formic acid water (B), gradient elution, flow rate 0.25 mL·min−1, and column temperature 45 °C. Quantitative analysis of the ingredients of Huojing Decoction was conducted.

Preparation of HJD Solution

HJD (Jiangyin Jiangtian Pharmaceutical, Suzhou, China) was obtained from Suzhou Hospital of Integrated Traditional Chinese and Western Medicine. The traditional Chinese medicine was identified by Zhang Genrong, the associate chief pharmacist of traditional Chinese medicine at Suzhou Hospital of Integrated Traditional Chinese and Western Medicine. The main ingredients were *Radix saposhnikoviae*(10g), *Ramulus cinnamomi*(10g), *Rhizoma et radix notopterygii*(6g), *Radix angelicae pubescentis*(10g), *Radix gentianae macrophyllae*(10g), *Rhizoma atractylodis*(10g), *Rhizoma atractylodis macrocephalae*(10g), *Arisaema cum bile* (6g), *Rhizoma pinelliae* (6g), totaling 9 Chinese medicine ingredients. The decoction of each component of the HJD (78g) was completely dissolved in 250mL of saline. After the processes of decoction and filtration, a suspension of the HJD with a concentration of 312mg/mL was prepared. Then, it was further concentrated to 78mL with a concentration of 1g/mL for subsequent use.

Animals and Ethical Statement

Sprague-Dawley (SD) rats (SCXK [Beijing] 2019–0010) were housed individually in separate cages within a quiet environment featuring 12-hour light and dark period (12L/12D 7:00–19:00). All animal subjects were provided with

sterilized feed and access to sterilized water. The experimental procedures commenced after a 7-day adaptation period. To conduct the experiments, a thorough manual on the care and handling of lab animals was utilized, along with ethical approval granted from the Suzhou Hospital of Integrated Chinese and Western Medicine's ethics committee(Approval Number: 2023041). Animal welfare was assessed according to Laboratory Animal-Guideline for Ethical Review of Animal Welfare (GB/T 35892–2018).

Establishment of Experimental KOA Model

Rats were anaesthetized initially with 4.0% isoflurane and maintained with 2.0–2.5% isoflurane. Following anesthesia with isoflurane, SD rats were secured on the operating table in supine position. Subsequently, 50μL of normal saline, dissolved with 3mg of sodium iodoacetate, was injected into the right knee cavity using a microsyringe. Upon regaining consciousness, the rats were placed in cages.

Administration of HJD

SD rats were randomly divided into six groups: Normal group (Normal), KOA group (KOA), Low dose group (HJD, 3g/kg) (Low), Medium dose group (HJD, 6g/kg) (Medium), High dose group (HJD, 12g/kg) (High), and Celecoxib group (Celecoxib, 50mg/kg). Each group consisted of 8 rats. Following the establishment of the model, the drug was administered once daily via intragastric administration for 14 consecutive days, with a dosage volume of 1mL per 100g of body mass.

Behavioral Assays

Behavioral Evaluation of Mechanical Allodynia

Paw withdrawal threshold (PWT) was measured with a von Frey wire to assess pain induced by mechanical touch. Von Frey filaments were employed to calculate the 50%-foot reduction threshold through the up-and-down method. Rats were placed in a 22cm ×12cm × 22cm organic glass box situated on a metal mesh for a duration of 30 minutes. Subsequently, the right hind foot sole of each rat was stimulated with von Frey filaments, ensuring a stimulation time of no less than 5 seconds. Measurements were taken continuously four times with von Frey filaments, with a 3-minute interval between each stimulation. The PWT of the rat was determined as the lowest mild response that was positive more than three times in five consecutive needling sessions.

Behavioral Evaluation of Thermal Hyperalgesia

The thermal radiation method was utilized to determine the paw withdrawal latency (PWL) in order to determine the heat pain threshold of the model rats. Rats were placed in a glass box for a 30-minute adaptation period. Utilizing the Hargreaves method, the soles of the rats were exposed to thermal stimulation. The PWL was recorded from the start of the stimulation until the rats lifted their feet to avoid the heat. In order to prevent tissue damage, the automatic cut-off time was established at 20 seconds. Each rat underwent 5 repetitions with a minimum 3-minute interval, and the PWL value was calculated as the average of the last 3 measurements. All behavioral experiments were conducted under double-blind conditions.

Weight Distribution (Static Weight Bearing)

Rats were positioned in a bipedal balance pain meter, and immediate changes in limb weight distribution occurred following knee joint injury. The pain level of the rats was assessed by measuring the difference in weights between hind limbs. Before the experiment, the instrument was calibrated, with the pedal was zero-adjusted in a no-load state and subsequently calibrated with a 500g weight. The experiment duration was set for 5 seconds. The experimental rat was secured in a specialized rat fixator, with its forelegs positioned on the fixator separator. The rat's head was placed in the black cage above. The left and right feet were then positioned in the center of the left and right pedals respectively. Pressing the start button initiated the recording of the left and right foot room payment pressure values, maximum

pressure values, and average pressure values during the measurement period when the rats were at rest. The average pressure value of rats in their resting state was recorded three times consecutively.

Immunohistochemical (IHC)

The DRG tissues were fixed in 4% paraformaldehyde at room temperature for 48h, and wrapped in a wax block. The sections were deparaffinized and rehydrated before incubation in antigen retrieval buffer. Hydrogen peroxide was applied to the sections, followed by blocking with BSA. Primer antibodies were sequentially added, and species-matching HRP-labeled secondary antibodies were applied. Utilizing DAB as the chromogen and hematoxylin as the counterstain, images were captured and semiquantitative analysis was performed by calculating the percentage of positive areas.

Immunofluorescence

The lumbar L4-L5 DRG tissues were fixed in 4% paraformaldehyde at room temperature for 48h, and wrapped in a wax block. Dehydration was followed by antigen retrieval of paraffin sections, and autofluorescence quencher and BSA were added sequentially. Finally, DAPI was used to stain the nuclei of the cells, and sections were observed and captured with the OLYMPUS IX73.

Immunoprecipitation

Homogenize the lumbar L4-L5 DRG tissue in a cold RIPA buffer containing a mixture of 1% PMSF and protease inhibitors. Centrifuge the dissolved tissue lysate at 12000 rpm for 15 minutes, and then collect the supernatant. Simultaneously prepare Protein A/G magnetic beads and add Tropomyosin receptor kinase A (TrkA) antibodies or normal rabbit IgG to the bead slurry to form a magnetic bead antibody complex. Subsequently, incubate the supernatant overnight with the bead-antibody complex at 4°C. After washing with elution buffer, boil the protein complex and perform protein blotting as previously described. Each sample should include a corresponding IgG control.

ELISA Assay

Levels of TNF-α, IL-6 and IL-1β were determined using enzyme-linked immunosorbent (ELISA) assay (EK382, EK306, EK301B MULTISCIENCES, China). On day 14, blood samples and DRG were gathered from all rats, and the concentrations of inflammatory mediators were analyzed based on the provided guidelines.

RNA Extraction and Quantitative Real-Time PCR Analysis (qRT-PCR)

DRG was used for the extraction of total RNA with the TRIzol reagent. Reverse transcription of 1 μg of RNA was carried out using the HiScript III All-in-one RT SuperMix Perfect for qRT-PCR (R333-01 Vazyme, China). A 20 μL volume was utilized for qRT-PCR, conducted in triplicate. The reaction mixture consisted of 10 μL of SYBR qRT-PCR Master Mix (Medicalbio, MR0321, China), 1 μL of diluted cDNA products, 0.4 μM of each paired primers, and 8.2 μL of deionized water. The levels of IL-1β, IL-6, and TNF-α were normalized to GAPDH, and quantification was carried out in accordance with the manufacturer's instructions. The primer sequences can be found in Table 1.

Table 1 The Primer Sequences Used in PCR

Gene	Primer	Primer Sequence [5'-3']
TNF-α	Forward	CGTCAGCCGATTTGCCATTT
	Reverse	CTCCAAAGTAGACCTGCCCG
IL-1β	Forward	AGCTTCAGGAAGGCAGTGTC
	Reverse	TCAGACAGCACGAGGCATTT
IL-6	Forward	AGAGACTTCCAGCCAGTTGC
	Reverse	ACAGTGCATCATCGCTGTTC
GAPDH	Forward	GACATGCCGCCTGGAGAAAC
	Reverse	AGCCCAGGATGCCCTTTAGT

Western Blot Analysis

A total of 48 rats were euthanized, and the lumbar L4-L5 DRG were collected and combined. The gathered tissues were lysed, and the resulting mixture was spun at 4 °C for 15 minutes at 12,000 r/min. The overall protein concentration was assessed, and equivalent quantities of proteins were divided on 10% polyacrylamide gels. For transferring fluid onto a PVDF membrane, a weak tris glycine 1 x buffer and 20% methanol were employed for 80 minutes at 200 mA. Subsequently, PVDF membranes were obstructed with 5% BSA mixed with Tris-buffered saline (TBS) for 60 minutes. The leading antibodies, such as TrkA (CST 2505 1:1000), p-TrkA (CST 4619 1:1000), Shc (CST 2432 1:1000), MKK3/6 (Santa Cruz Biotechnology sc-136982 1:1000), p-MKK3/6 (CST 12280 1:1000), p38 (CST 8690 1:1000), p-p38 (CST 4511 1:1000), CGRP (Santa Cruz Biotechnology sc-57053 1:1000), TRPV1 (Abcam ab203103 1:1000), GAPDH(CST 5174 1:5000), Anti-rabbit IgG (H+L)(CST 14708 1:3000), Anti-mouse IgG (H+L)(CST14709 1:3000). TBST was employed to cleanse the membranes four times for five minutes per round. HRP-coupled subsequent antibodies (ZENBIO 511203, 1:7500) were exposed for one hour at ambient temperature on the membranes. Eventually, the membrane was visualized using a Tanon scan imager after ECL (Medicalbio, PT01001) reagent visualization. For the quantification of Western blots, GAPDH was utilized as a benchmark for normalizing protein expression.

Statistical Analysis

Mean values with corresponding standard deviations (Mean ± SD) were obtained from a minimum of three separate experiments. Utilizing GraphPad Prism 8 software (USA), statistical evaluations were performed. Differences between groups were evaluated either through one-way ANOVA with Bonferroni corrections or two-way ANOVA with Bonferroni corrections. Statistical significance was defined as a p-value less than 0.05.

Results

Network Pharmacology

After searching in the TCMSP database, we identified 46 HJD-related targets. Subsequently, we selected a total of 2786 KOA-related targets using GeneCards and OMIM databases. Finally, we confirmed the correlation of 54 targets with Huojing Tang and knee arthritis (Figure 1A). The core targets in the constructed protein-protein interaction (PPI) network include JUN, IL-6, MAPK14(p38) and other genes (Figure 1B). According to the gene enrichment analysis of GO and KEGG databases, HJD treatment of KOA may be related to the MAPKs signaling pathway (Figure 1C and D). Component-disease-pathway-target network diagram. Purple represents HJD components and green represents disease genes related to KOA (Figure 1E).

Analysis of Main HJD Components by UPLC-MS/MS

The main components of HJD were analyzed using UPLC-MS/MS, and the total ion chromatograms in both positive and negative ion modes were obtained (Figure 2). In both ion modes, the chromatographic peaks of the main components in HJD were relatively abundant. Based on the mass spectrometry data, the ion modes, parent ions, and daughter ions of each main component were determined. Qualitative analysis of the main components in HJD was performed by referring to relevant literature information and considering the fragmentation patterns of the compounds. A total of 27 compounds were identified and verified using reference standards (Table 2).

HJD Dose-Dependently Protects Knee Joint in Rats After MIA Injection

MIA was injected to the rat to induce KOA model. On the 4th post-injection, we assessed the damage to the knee joints of rats. An image of the rat knee joint illustrates the damage following MIA injection (Figure 3A). To further evaluate knee joint injury, Hematoxylin and eosin (H&E) staining was applied to detect damage in each rat's knee joint. The results revealed severe cartilage damage in KOA rats. Conversely, intragastric injection of HJD dose-dependent dependently rescued the cartilage damage in the knee joint (Figure 3B). In addition, femoral micro-computed tomography, along with bone volume and bone surface statistics, were used to observe damage to the rat knee joint. The results showed that intragastric injection of HJD delayed knee joint damage in a dose-dependent manner (Figure 3C–E). These findings indicate that HJD can dose-dependently protect knee joint in rats following MIA injection.

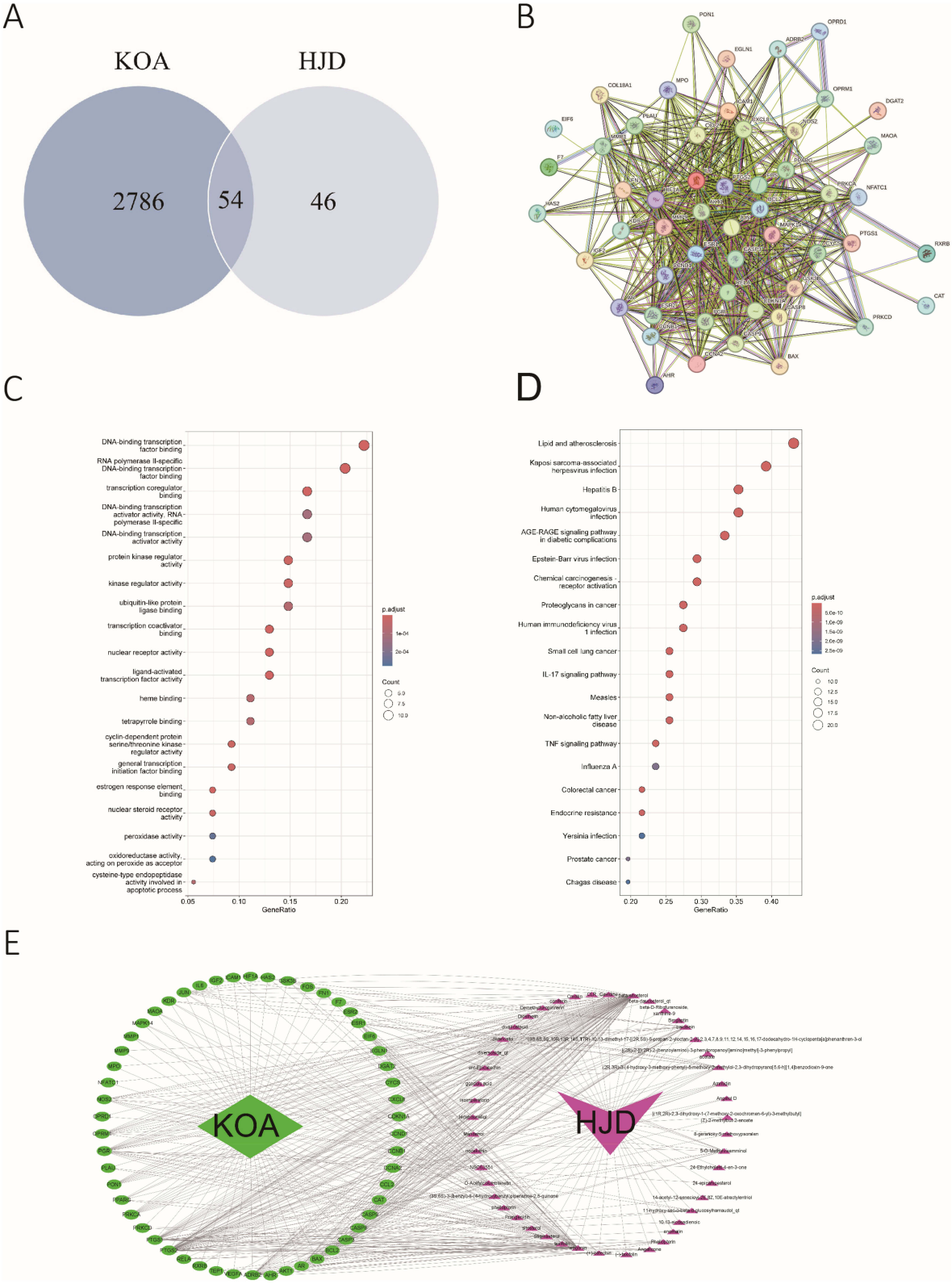

Figure 1 Network pharmacology of HJD. (**A**) Venn diagram; (**B**) PPI network; (**C**) GO enrichment analysis; (**D**) KEGG enrichment analysis; (**E**) Component-disease-pathway-target network.

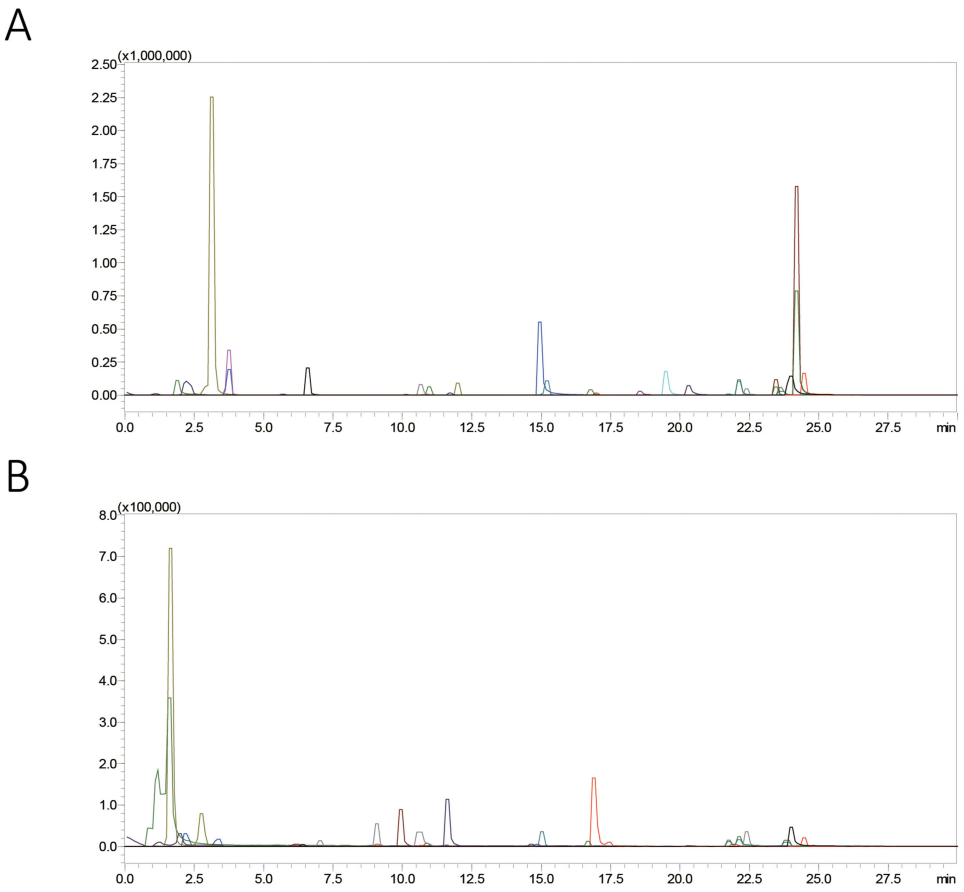

Figure 2 Analysis of main HJD components by UPLC-MS/MS. (**A**) The MRM ion chromatogram of the reference substance (overlay plot). (**B**) The MRM ion chromatogram of the test sample (overlay plot).

HJD Alleviated Pain Behavior and Suppressed the Increases of CGRP and TRPV1 in DRG in a Dose-Dependent Manner

Subsequent investigations were conducted on mechanical allodynia and thermal hyperalgesia in rats post MIA injection. The results shown in Figure 4 indicated a significant decrease in the mechanical threshold ($P < 0.01$, Figure 4A), PWL in response to heat stimulation ($P < 0.01$, Figure 4B), and weight bearing ($P < 0.01$, Figure 4C) 4 days after the MIA injection, with the

Table 2 Qualitative Analysis of HJD

NO.	RT/ min	PoundCom	Chemical Formula	Molecular Weight	Ion mode	Parent ion	Fragment ions	CE	Component Attribution
1	1.110	Uracil	C4H4N2O2	112.09	[M-H]-	111.10	42.05; 80.05	22	Rhizoma pinelliae
2	1.648	Citric acid	C6H8O7	192.14	[M-H]-	191.30	111.15; 87.05	12	Rhizoma pinelliae
3	2.018	Uridine	C9H12N2O6	244.20	[M+HCOO]-	289.10	243.20; 200.20	10	Rhizoma pinelliae
4	2.758	Adenosine	C10H13N5O4	267.24	[M+H]+	268.15	136.20;119.05	20	Rhizoma pinelliae
5	3.430	Inosine	C10H12N4O5	268.23	[M-H]-	267.30	135.20; 108.15	20	Rhizoma pinelliae
6	3.430	Guanosine	C10H13N5O5	283.24	[M-H]-	282.25	150.20; 133.20	17	Rhizoma pinelliae
7	6.390	Caffeic acid	C7H6O4	154.12	[M-H]-	153.30	109.20;108.15	17	Ramulus cinnamomi
8	9.955	Hyperoside	C16H24O10	376.36	[M-H]-	375.25	213.25;169.30	16	Gentiana Macrophylla Pall
9	10.661	Chlorogenic acid	C16H18O9	354.31	[M-H]-	353.10	191.25;85.10	19	Rhizoma et radix notopterygii

(*Continued*)

Table 2 (Continued).

NO.	RT/ min	PoundCom	Chemical Formula	Molecular Weight	Ion mode	Parent ion	Fragment ions	CE	Component Attribution
10	10.762	Crocetin	C27H32O16	612.53	[M-H]-	611.20	325.20;491.15	26	Ramulus cinnamomi
11	10.897	Scutellarein-7-O-glucoside	C16H22O10	374.34	[M+HCOO]-	419.05	179.25;89.10	13	Gentiana Macrophylla Pall
12	11.603	Gentiopicroside	C16H20O9	356.32	[M+HCOO]-	401.10	179.25; 45.10	13	Gentiana Macrophylla Pall
13	11.839	Swertiapuniside	C16H22O9	358.34	[M+HCOO]-	403.25	195.30; 125.20	14	Gentiana Macrophylla Pall
14	14.899	Scopolin	C10H8O4	192.17	[M-H]-	191.35	176.20;104.15	16	Radix Angelicae Biseratae
15	15.067	Ferulic acid	C10H10O4	194.18	[M-H]-	193.35	134.15;178.25	17	Rhizoma et radix notopterygii
16	16.715	Ligustilide	C16H18O6	306.32	[M+H]+	307.15	235.05;259.05	27	Rhizoma et radix notopterygii
17	16.917	Fraxetin-7-O-glucoside	C20H24O9	408.40	[M+HCOO]-	453.10	227.20;407.20	20	Rhizoma et radix notopterygii
18	18.531	Baicalin	C21H18O11	446.32	[M-H]-	445.05	269.20;113.20	21	Rhizoma et radix notopterygii
19	19.439	Wogonoside	C22H20O11	460.39	[M-H]-	459.00	268.10;283.15	32	Rhizoma et radix notopterygii
20	20.314	Tetrahydroxypropyl-benzene	C11H6O3	186.16	[M+H]+	187.05	131.10;115.10	26	Radix Angelicae Biseratae
21	22.130	Deoxycholic acid	C24H40O4	392.58	[M+HCOO]-	437.30	391.35; 45.05	19	Arisaema cum bile
22	22.433	Alisol A lactone III	C15H20O3	248.32	[M+HCOO]-	293.20	236.25; 221.35	14	Rhizoma atractylodis
23	23.442	Eupatilin	C16H14O4	270.28	[M+H]+	271.10	203.10;147.15	18	Rhizoma et radix notopterygii
24	23.778	Cholic acid	C24H40O4	392.57	[M+HCOO]-	437.25	391.35; 45.10	20	Arisaema cum bile
25	24.047	Rutaecarpine	C15H16O3	244.29	[M+H]+	245.10	189.05;131.15	16	Radix Angelicae Biseratae
26	24.249	Isoscutellarein	C16H14O4	270.28	[M+H]+	271.10	203.10;147.15	15	Radix Angelicae Biseratae
27	24.484	Dehydroisoandrosterone	C19H20O5	328.36	[M+H]+	329.15	187.05;229.10	25	Radix Angelicae Biseratae

sensitivity remaining constant for 14 consecutive days in rats. In contrast, HJD demonstrated a dose-dependent alleviation of mechanical allodynia ($P < 0.05$, Figure 4A), thermal hyperalgesia ($P < 0.05$, Figure 4B), and weight bearing ($P < 0.05$, Figure 4C) in rats post MIA injection. Noteworthy is that Celecoxib, a well-established analgesic compound, substantially increased the mechanical threshold (Figure 4A), PWL in response to heat stimulation (Figure 4B), and weight bearing (Figure 4C) in MIA rats as well. Furthermore, the results highlighted that the analgesic effect of a high dose of HJD is similar to that of celecoxib. Subsequent examination was carried out on the expression levels of CGRP and TRPV1 in rat DRG from each group. The DRG of the KOA rats exhibited more intense CGRP and TRPV1 staining compared to the normal model, while DRG tissue revealed a lighter CGRP and TRPV1 staining after treatment with HJD (Figure 4D–F). Additionally, Western blot results indicated that HJD treatment significantly inhibited the increased protein levels of TRPV1 and CGRP (Figure 4G–I).

TrkA Signaling Pathway is Involved in the Amelioration of HJD on Knee Joint Pain in KOA Rats

TrkA is transported to the DRG by endoaxon and influences the expression and activation of TRPV 1 in DRG through P38 pathway.[19] We observed p-TrkA in DRG using immunofluorescence, where the fluorescence intensity of p-TrkA in KOA rats

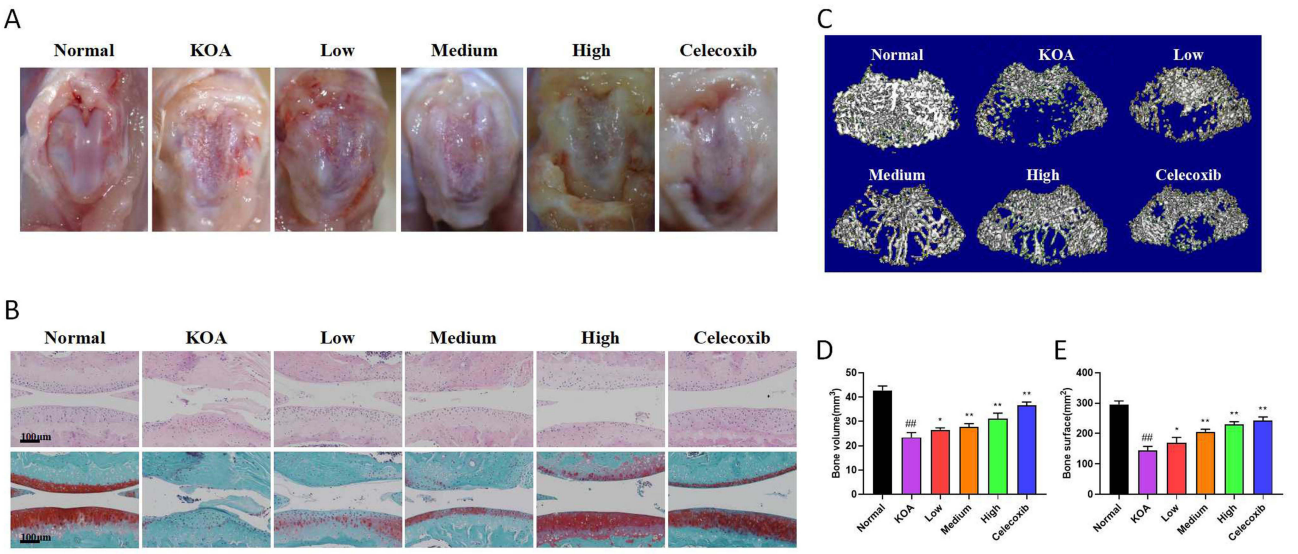

Figure 3 HJD dose-dependently protected knee joint in rats after MIA injection. (**A**) Morphological images of rat knee joint; (**B**) H&E and Safranin O staining images of knee joint; (**C**) Micro-computed tomography images of femur; (**D-E**) Statistical analysis of bone volume (**D**) and bone surface (**E**). Inter-group differences were assessed using two-way repeated ANOVA with Bonferroni corrections. $^{\#\#}p<0.01$ vs Normal group, $^{*}p<0.05$ vs KOA group, $^{**}p<0.01$ vs KOA group.

was higher than that in normal. Conversely, the fluorescence intensity of p-TrkA in DRG with HJD treatment was lighter than KOA rats (Figure 5A–B). Additionally, we detected the expression of TrkA and p-TrkA protein in the DRG by Western blot. Our results indicated that HJD treatment significantly inhibited the increase of p-TrkA (Figure 5C). Statistical analysis results demonstrated that KOA induced a significant up-regulation of p-TrkA expression ($P < 0.01$, Figure 5D). Taken together, these results suggest that HJD may inhibit the upregulation of p-TrkA in DRG of KOA rats.

HJD suppressed the up-regulation of p38 and MKK3/6 by inhibiting the binding of TrkA and Shc in the DRG of KOA rats

We proceeded to examine the protein expression of p38 and MKK3/6 in the DRG of KOA rats after treatment with HJD. Our results demonstrated that MIA induced a significant increase of the protein bands of p-p38 and p-MKK3/6, while HJD treatment significantly suppressed these increases (Figure 6F). Statistical analysis results revealed a significant up-regulation of the protein expression of p-p38 and p-MKK3/6 induced by MIA. Additionally, HJD treatment significantly suppressed this up-regulation ($P<0.05$, Figure 6G–H). Subsequently, we observed p-p38 in DRG by immunofluorescence, where the fluorescence intensity of p-p38 in DRG of KOA was higher than that in normal group. Conversely, the fluorescence intensity of p-p38 in DRG with HJD treatment was lighter than KOA rats ($P < 0.01$, Figure 6D–E). Taken together, these results suggested that HJD may suppress the phosphorylation of p38 and MKK3/6 in DRG of KOA rats.

We used immunofluorescence colocalization and co-immunoprecipitation technology to further detect the expression of TrkA and Shc in the DRG. Our results showed that HJD significantly inhibited the binding of TrkA and Shc (Figure 6A–C). These findings collectively suggest that HJD may inhibit the upregulation of TrkA in the DRG of KOA rats, thereby inhibiting the binding of TrkA and Shc.

HJD May Relieve Pain in KOA Rats Through Suppression the Levels of IL-1β, IL-6 and TNF-α

We conducted a serum analysis of IL-1β, IL-6 and TNF-α in rats to evaluate the impact of HJD on these cytokine levels. Following MIA injection, there was significant increase in IL-1β ($P < 0.01$, Figure 7A), TNF-α ($P < 0.01$, Figure 7B) and IL-6 ($P < 0.01$, Figure 7C) levels. Conversely, HJD exhibited a significant dose-dependent suppression of IL-1β ($P < 0.05$, Figure 7A), TNF-α ($P < 0.05$, Figure 7B) and IL-6 ($P < 0.05$, Figure 7C) in KOA rats. These findings suggested that HJD may potentially alleviate pain in KOA rats by suppressing IL-1β, IL-6 and TNF-α levels.

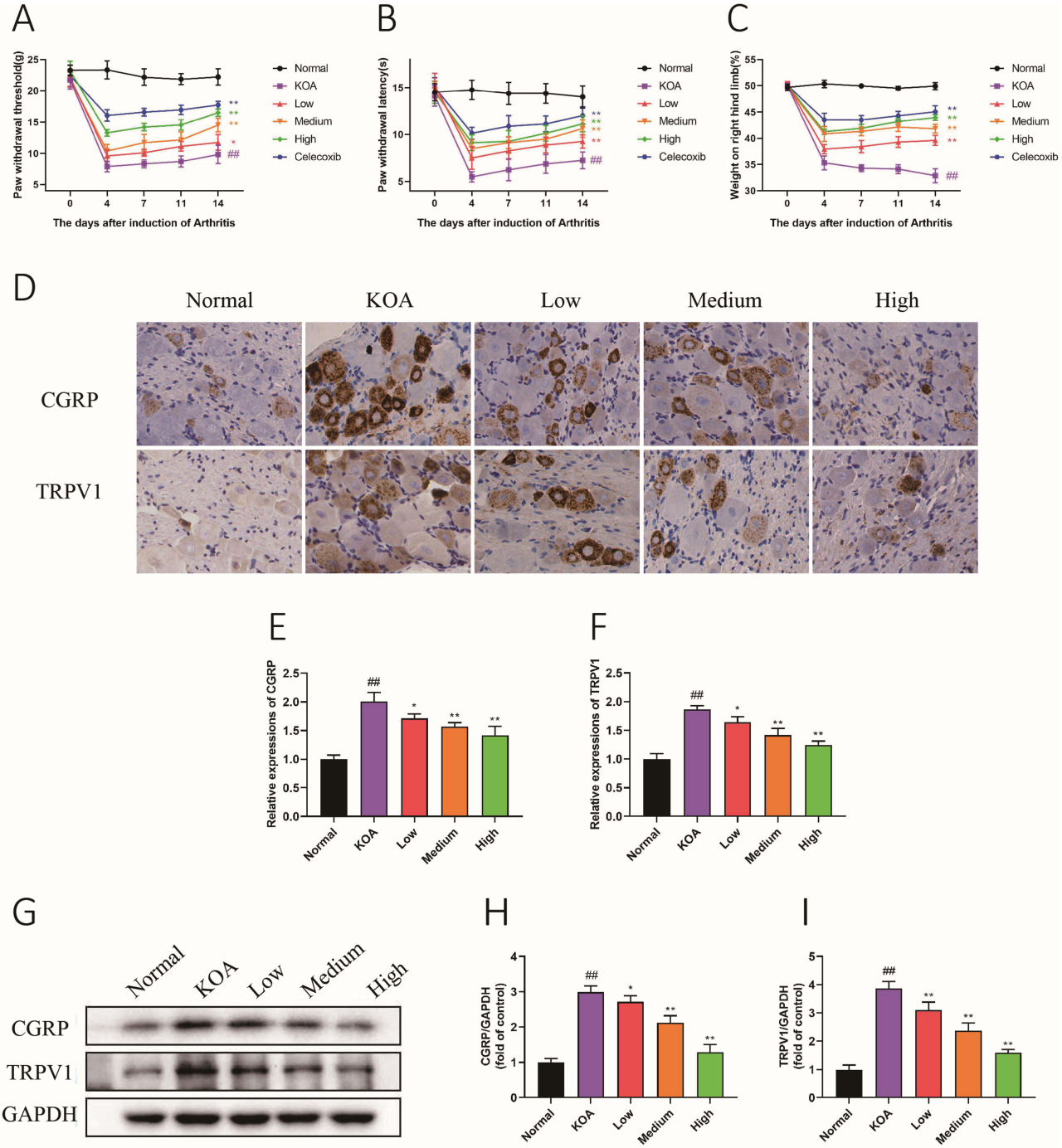

Figure 4 HJD alleviates pain in a dose-dependent manner. (**A**) Paw withdrawal mechanical threshold, (**B**) paw withdrawal thermal latency, and (**C**) hind limb weight distribution in rats from each group. (**D-F**) Immunohistochemical detection of CGRP and TRPV1 in the DRG of each. (**G-I**) Western blot analysis of CGRP and TRPV1 levels in the DRG. Inter-group differences were assessed using two-way repeated ANOVA with Bonferroni corrections. $^{\#\#}p<0.01$ vs Normal group, $^{*}p<0.05$ vs KOA group, $^{**}p<0.01$ vs KOA group.

Additionally, we explored the mechanistic insights by examining the mRNA expression of IL-1β, IL-6 and TNF-α in the DRG of rats post-HJD treatment. MIA induction significantly up-regulated the expressions of IL-1β, TNF-α and IL-6 ($P < 0.01$, Figure 7D–F). In contrast, HJD treatment significantly inhibited this up-regulation ($P < 0.05$, Figure 7D–F).

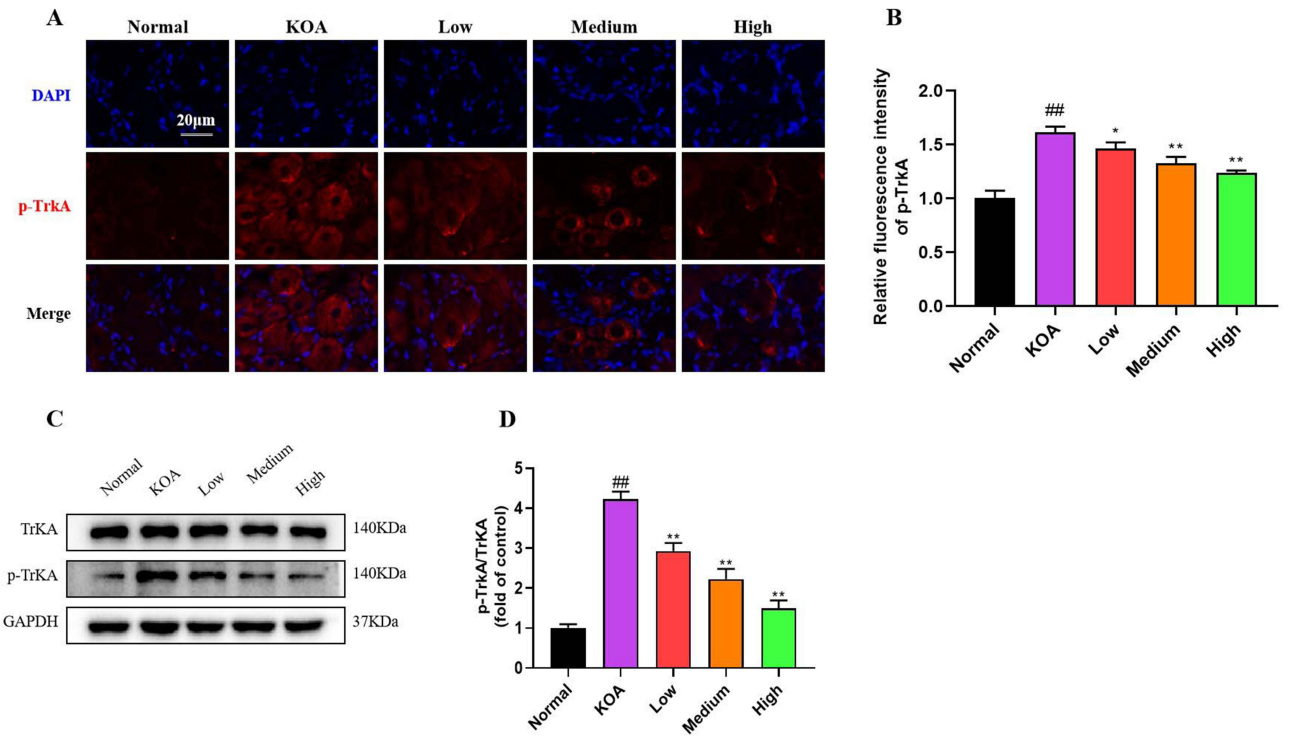

Figure 5 TrkA signaling pathway is involved in the amelioration of knee joint pain by HJD in KOA rats. (**A**) and (**B**) Immunofluorescence staining showing p-TrkA expression in the DRG of each group; (**C**) and (**D**) Western blot analysis depicting the p-TrkA expression in the DRG of each group. Inter-group differences were assessed using one-way repeated ANOVA with Bonferroni corrections. ## p<0.01 vs Normal group, *p<0.05 vs KOA group, **p<0.01 vs KOA group.

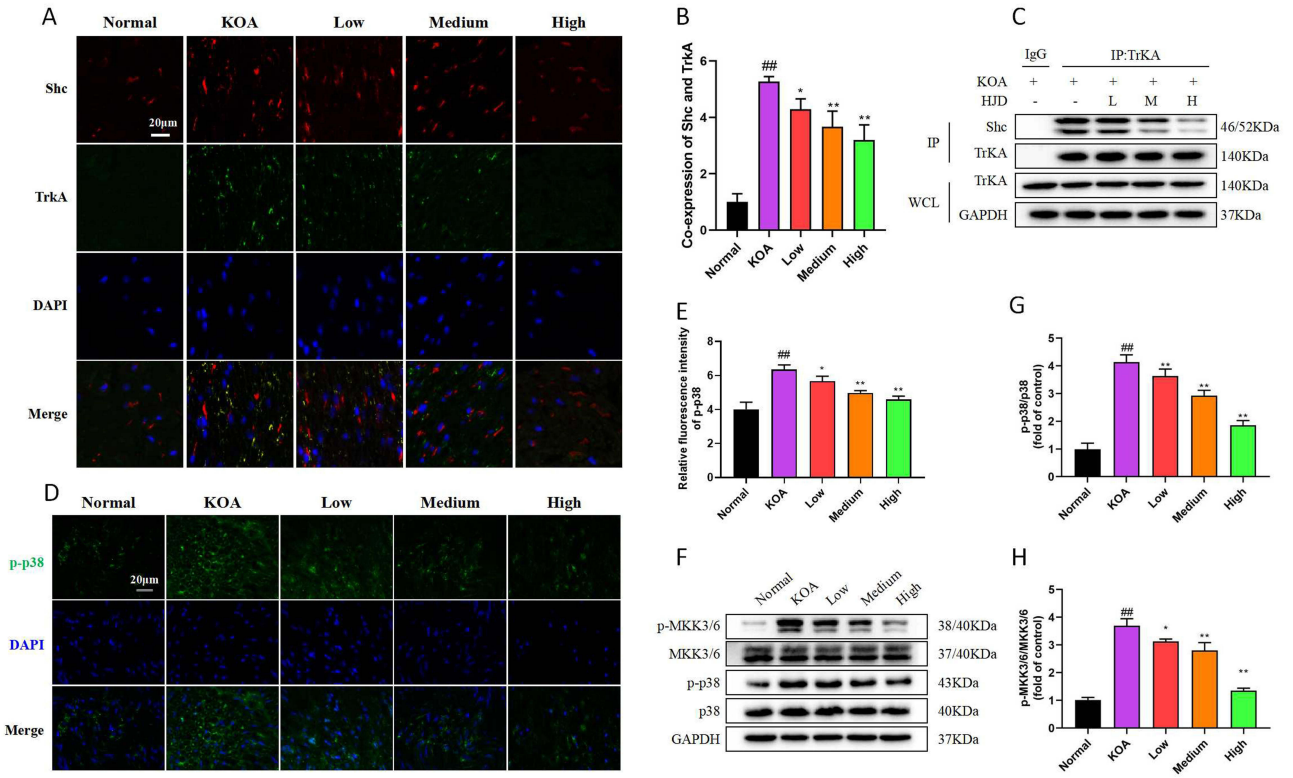

Figure 6 HJD suppressed the up-regulation of p38 and MMK3/6 by inhibiting the binding of TrkA and Shc in the DRG of KOA rats. (**A**) and (**B**) The immunofluorescence colocalization of TrkA and Shc. (**C**) Representative Western blots for immunoprecipitation of TrkA and Shc. (**D**) and (**E**) Immunofluorescence staining depicting p-p38 in the DRG of each group. (**F-H**) Expression level of p-p38, p-MKK3/6 expression. Inter-group differences were assessed using one-way repeated ANOVA with Bonferroni corrections. ## P<0.01vs. Normal group, *p<0.05 vs KOA group, ** P<0.01 vs KOA group.

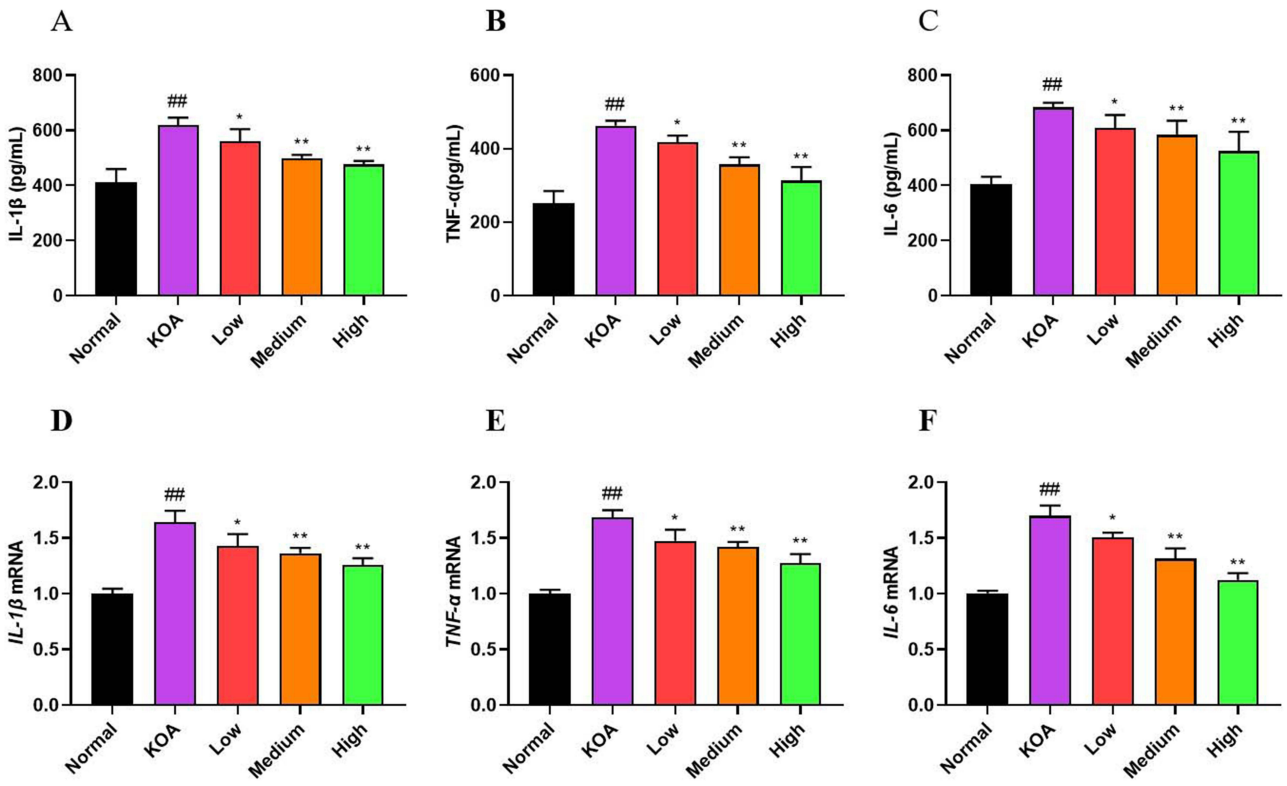

Figure 7 HJD may relieve joint knee pain in KOA rats through suppression the levels of IL-1β, TNF-α and IL-6. (**A**) Serum levels of the inflammatory factor IL-1β were determined by ELISA. (**B**) Serum levels of inflammatory factor TNF-αwere determined by ELISA. (**C**) Serum levels of the inflammatory factor IL-6 were determined by ELISA. (**D-F**) The mRNA expression of IL-1β, TNF-α and IL-6 in the DRG of rats. High and Medium group were compared with KOA group. Inter-group differences were assessed using one-way repeated ANOVA with Bonferroni corrections. $^{\#\#}p<0.01$ vs Normal group, $^{*}p<0.05$ vs KOA group, $^{**}p<0.01$ vs KOA group.

Discussion

Previous studies have demonstrated that MIA induced KOA pain results in decreased weight bearing, mechanical allodynia and thermal hyperalgesia.[20] However, the causes of KOA pain are complex, and the transmission of pain signals involves intricate processes. The primary mechanism involves promoting or suppressing signal changes. As of now, the relationship between pain signals and pain are not fully understood.[21]

Reviewed studies indicated that the cartilage degeneration occurs during the course of KOA. In this pathogenic process, the release of inflammatory cytokines, namely TNF-α, IL-1β and IL-6, plays a significant role. Correspondingly, levels of these inflammatory factors would decrease after treatment.[22] Another study demonstrated that suppressing the expression of the p38 signaling pathway in MIA-induced KOA rats could reduce IL-1β and IL-6.[23] TNF-α, present in osteoarthritis lesions, can induce chondrocyte apoptosis. The main mechanism involves TNF-α-induced upregulation of p38, leading to chondrocyte apoptosis and oxidative damage. Inhibiting the p38 signaling pathway has been shown to improve cartilage damage in osteoarthritis.[24] One study demonstrated that specific p38 phosphorylation in DRG was identified in a pain model of MIA-induced OA. The model exhibited central sensitization, with high expression of p38 phosphorylation in the DRG. The findings of this study suggested that the activation of p38 could induce the occurrence of pain sensitization in osteoarthritis, and the pain could be alleviated by inhibiting MAPK activation.[20] MKK3 and MKK6 act as the upstream of p38, regulating its function. MKK3 primarily mediates osteoclast formation, while MKK6 promotes the production of inflammatory cytokines.[25] Research has shown that the p38 plays a crucial role in the progression of OA. Studies conducted on chondrocytes affected by OA in humans have indicated that MKK3 plays a significant role in activating the p38 signaling pathway. More specifically, the activation of MKK3 is responsible for triggering the activation of p38. Experimental data has demonstrated that the downstream target p38 can be effectively inhibited by preventing the activation of MKK3.[26] In a murine study, it was observed that the inhibition of upstream kinases (MKK3 or MKK6) in the p38 pathway contributes to the regression of arthritis. This intervention led to

a reduction in the expression of synovial inflammatory mediators. The utilization of blockers targeting the upstream kinase of p38 exhibited a significant inhibitory effect on the expression of inflammatory cytokines and MAPK.[27] Meanwhile, the study has indicated that MKK3/6 are the upstream activators of p38, which can give rise to the phosphorylation of p38 and be associated with the emergence and sustenance of pain.[28] In normal chondrocytes, nearly no expression of TrkA was detected. However, variations in TrkA expression were noted in osteoarthritis chondrocytes with varying degrees of injury. Notably, more severe bone and joint injuries were associated with increased TrkA expression in chondrocytes.[29] Moreover, the experimental findings suggest that the blockade TrkA holds promise as a potential target for OA pain relief.[30] Inflammation is a key element of pain associated with arthritis, and nerve growth factor (NGF) plays a significant role in both acute and chronic pain states. Furthermore, NGF is intricately linked to inflammation-related pain. NGF exerts its effects through the TrkA. Since OA-induced pain is primarily driven by inflammation in which NGF plays a central role. The inhibition of TrkA has demonstrated significant potential in ameliorating pain behavior in experimental rat models.[31] TrkA plays pivotal roles in numerous physiological processes within the nervous system. Specifically, Shc competes for Trk receptor binding, potentially resulting in the activation of the downstream MAPK signaling pathway.[32,33] Studies have demonstrated that activating TrkA specifically decreases mechanical allodynia and thermal hyperalgesia via the p38 pathway.[34] Additionally, the activation of TrkA in DRG has been linked to the upregulation of TRPV1 channels.[35] The positive innervation of TRPV1 can be inhibited and hyperalgesia can be improved by intervening in TrkA.[36] Furthermore, the TrkA pathway has been linked to enhancing the release of CGRP at the far end of the spinal cord. The released CGRP is then transported to the dorsal horn of the spinal cord. Where it binds to receptors and facilitates the initiation of mid-level sensitization.[37] Additionally, TRPV1 plays a crucial role in triggering inflammatory immune responses and controlling pain levels. Numerous studies have underscored the closes association between TRPV1 and pain in conditions characterized by chronic pain.[38] Moreover, TRPV1 is expressed in joint tissues, and its expression of synovial tissues is notably increased in KOA. Inhibition of TRPV1 expression has been demonstrated to ameliorate the inflammatory pain associated with OA.[39] In a simulation of unplanned discomfort induced by a TRPV1 stimulant, it was determined that the stimulation of TRPV1 in DRG nerve cells triggers the discharge of CGRP. Subsequently, the release gives rise to mechanical hyperalgesia, thermal hyperalgesia, and alterations in weight distribution.[18]

Building upon the aforementioned findings, we observed that the analgesic effect of HJD is primarily manifest through the suppression of CGRP and TRPV1 expression. Additionally, our findings indicate that HJD exhibits effective analgesic and anti-inflammatory by downregulating the TrkA/MKK3/6/p38 Pathway. To deepen our understanding, we further investigated the interplay between TrkA/MKK3/6/p38, TRPV1 and CGRP. The outcomes suggest that HJD downregulates the expression of CGRP and TRPV1 by suppressing the TrkA/MKK3/6/p38 Pathway. Despite these promising findings, our study is subject to certain limitations. For instance, it features a relatively small sample size and focuses solely on the MIA model. Future undertakings will encompass the expansion of the sample size, the exploration of diverse animal models, and the employment of advanced methodologies for investigating additional aspects of chronic pain associated with KOA.

Conclusions

In summary, this study investigated the analgesic effects and underlying mechanism of HJD on KOA based on a combination of network pharmacology and experimental verification. In addition, the main components of HJD were analyzed by UPLC-MS/MS. It reveals that HJD emerges as promising therapeutic intervention for KOA pain. Its demonstrated efficacy in alleviating allodynia and hyperalgesia in rats with KOA suggests a potential avenue for pain management. This effect is likely attributed to the down-regulation of the TrkA/p38/MKK3/6 signaling cascade in DRG and the modulation of the serum inflammatory cytokines, namely IL-1β, IL-6 and TNF-α. Taken together, the findings underscore the promising analgesic and bone protection effects of HJD in the context of KOA.

Abbreviations

OA, Osteoarthritis; KOA, Knee osteoarthritis; Interleukin, IL; TNF, Tumor necrosis factor; IL-1β, Interleukin-1β; IL-6, Interleukin-6; TNF-α, Tumor necrosis factor-α; DRG, Dorsal root ganglion; p38, P38 mitogen activated protein kinase;

MIA, Monoiodoacetic acid; MIA-OA, MIA-induced osteoarthritis; TRPV1, Transient receptor potential vanilloid 1; CGRP, Calcitonin gene-related peptide; TCMSP, The Pharmacology of Traditional Chinese Medicine Systems; OMIM, Online Mendelian Inheritance in Man; HJD, Huojing Decoction; PPI, Protein-Protein Interaction; GO, Gene Ontology; KEGG, Kyoto Encyclopedia of Genes and Genomes; UPLC-MS/MS, Ultra-high performance liquid chromatography-tandem mass spectrometry; SD, Sprague-Dawley; PWT, Paw withdrawal threshold; PWL, Paw withdrawal latency; IHC, Immunohistochemical; ELISA, Enzyme-linked immunosorbent assay; qRT-PCR, Quantitative Real-Time PCR; TrkA, Tropomyosin receptor kinase A; H&E, Hematoxylin and eosin; NGF, Nerve growth factor.

Data Sharing Statement

All data generated or analysed during this study are included in this published article.

Acknowledgments

Xinchao Jiang and Yinyin Guo are co-first authors for this study. This paper has been uploaded to ResearchGate as a preprint: https://www.researchgate.net/publication/381304901_Suppression_of_CGRP_and_TRPV1_Expression_in_Dorsal_Root_Ganglia_of_Knee_Osteoarthritis_Rats_by_Huojing_Decoction_via_TrkAMKK36p38_Pathway. Thanks to the staff of the Central Laboratory of Suzhou Hospital of Integrated Traditional Chinese and Western Medicine.

Funding

This study was supported by the Youth Programs of the Wuzhong District Department of Science and Technology (WZYW2021014); Suzhou Integrated Traditional Chinese and Western Medicine Research Fund Project (SKYD2023245); Jiangsu Traditional Chinese Medicine Science and Technology Development Project (MS2023095); Suzhou Science and Technology Project (SKJYD2021212); Suzhou Science and Technology Project (SKJYD2021032).

Disclosure

The authors declare that they have no competing interests in this work.

References

1. Farinelli L, Riccio M, Gigante A, De Francesco F. Pain management strategies in osteoarthritis. *Biomedicines*. 2024;12(4):805. doi:10.3390/biomedicines12040805
2. Nelson A. Osteoarthritis year in review 2017: clinical. *Osteoarthritis Cartilage*. 2018;26(3):319–325. doi:10.1016/j.joca.2017.11.014
3. Liang Y, Xu Y, Zhu Y, Ye H, Wang Q, Xu G. Efficacy and safety of Chinese herbal medicine for knee osteoarthritis: systematic review and meta-analysis of randomized controlled trials. *Phytomedicine*. 2022;100:154029. doi:10.1016/j.phymed.2022.154029
4. Zhao X, Meng F, Hu S, et al. The synovium attenuates cartilage degeneration in KOA through activation of the Smad2/3-Runx1 cascade and chondrogenesis-related miRNAs. *Mol Ther Nucleic Acids*. 2020;22:832–845. doi:10.1016/j.omtn.2020.10.004
5. He B, Tao H, Liu S, et al. Carboxymethylated chitosan protects rat chondrocytes from NO-induced apoptosis via inhibition of the p38/MAPK signaling pathway. *Mol Med Rep*. 2016;13(3):2151–2158. doi:10.3892/mmr.2016.4772
6. Li J, Shao Q, Zhu X, Sun G. Efficacy of autologous bone marrow mesenchymal stem cells in the treatment of knee osteoarthritis and their effects on the expression of serum TNF-α and IL-6. *J Musculoskelet Neuronal Interact*. 2020;20(1):128–135.
7. Sun Z, Su W, Wang L, Cheng Z, Yang F. Clinical effect of bushen huoxue method combined with platelet-rich plasma in the treatment of knee osteoarthritis and its effect on IL-1, IL-6, VEGF, and PGE-2. *J Healthc Eng*. 2022;2022:9491439. doi:10.1155/2022/9491439
8. Pang Y, Zhao L, Ji X, Guo K, Yin X. Analyses of Transcriptomics upon IL-1β-stimulated mouse chondrocytes and the protective effect of catalpol through the NOD2/NF-κB/MAPK signaling pathway. *Molecules*. 2023;28(4):1606. doi:10.3390/molecules28041606
9. Xu M, Wu R, Zhang L, et al. Decreased MiR-485-5p contributes to inflammatory pain through post-transcriptional upregulation of ASIC1 in rat dorsal root ganglion. *J Pain Res*. 2020;13:3013–3022. doi:10.2147/JPR.S279902
10. Mai L, Zhu X, Huang F, He H, Fan W. p38 mitogen-activated protein kinase and pain. *Life Sci*. 2020;256:117885. doi:10.1016/j.lfs.2020.117885
11. Yang Y, Zhou W, Xu X, et al. Aprepitant inhibits JNK and p38/MAPK to attenuate inflammation and suppresses inflammatory pain. *Front Pharmacol*. 2021;12:811584. doi:10.3389/fphar.2021.811584
12. Lee Y, Pai M, Brederson J, et al. Monosodium iodoacetate-induced joint pain is associated with increased phosphorylation of mitogen activated protein kinases in the rat spinal cord. *Molecular Pain*. 2011;7:39. doi:10.1186/1744-8069-7-39
13. Yu C, Li P, Wang Y, Zhang K, Zheng Z, Liang L. Sanguinarine attenuates neuropathic pain by inhibiting P38 MAPK activated neuroinflammation in rat model. *Drug Des Devel Ther*. 2020;14:4725–4733. doi:10.2147/DDDT.S276424
14. Sanna M, Stark H, Lucarini L, Ghelardini C, Masini E, Galeotti N. Histamine H4 receptor activation alleviates neuropathic pain through differential regulation of ERK, JNK, and P38 MAPK phosphorylation. *Pain*. 2015;156(12):2492–2504. doi:10.1097/j.pain.0000000000000319
15. Koda K, Hyakkoku K, Ogawa K, et al. Sensitization of TRPV1 by protein kinase C in rats with mono-iodoacetate-induced joint pain. *Osteoarthritis Cartilage*. 2016;24(7):1254–1262. doi:10.1016/j.joca.2016.02.010

16. Arai T, Suzuki-Narita M, Takeuchi J, et al. Analgesic effects and arthritic changes following intra-articular injection of diclofenac etalhyaluronate in a rat knee osteoarthritis model. *BMC musculoskelet Disord*. 2022;23(1):960. doi:10.1186/s12891-022-05937-y
17. Peng J, Gu Y, Wei J, et al. LncRNA MEG3-TRPV1 signaling regulates chronic inflammatory pain in rats. *Molecular Pain*. 2022;18:17448069221144246. doi:10.1177/17448069221144246
18. Fattori V, Zaninelli T, Ferraz C, et al. Maresin 2 is an analgesic specialized pro-resolution lipid mediator in mice by inhibiting neutrophil and monocyte recruitment, nociceptor neuron TRPV1 and TRPA1 activation, and CGRP release. *Neuropharmacology*. 2022;216:109189. doi:10.1016/j.neuropharm.2022.109189
19. Puntambekar P, Mukherjea D, Jajoo S, Ramkumar V. Essential role of Rac1/NADPH oxidase in nerve growth factor induction of TRPV1 expression. *J Neurochem*. 2005;95(6):1689–1703. doi:10.1111/j.1471-4159.2005.03518.x
20. Sun L, Wang G, He M, Mei Z, Zhang F, Liu P. Effect and mechanism of the CACNA2D1-CGRP pathway in osteoarthritis-induced ongoing pain. *Biomed Pharmacother*. 2020;129:110374. doi:10.1016/j.biopha.2020.110374
21. Carlesso L, Law L, Wang N, Nevitt M, Lewis C, Neogi T. Association of pain sensitization and conditioned pain modulation to pain patterns in knee osteoarthritis. *Arthritis Care Res (Hoboken)*. 2022;74(1):107–112. doi:10.1002/acr.24437
22. Nambi G. Does low level laser therapy has effects on inflammatory biomarkers IL-1β, IL-6, TNF-α, and MMP-13 in osteoarthritis of rat models-A systemic review and meta-analysis. *Lasers Med Sci*. 2021;36(3):475–484. doi:10.1007/s10103-020-03124-w
23. Zheng S, Ren J, Gong S, Qiao F, He J. CTRP9 protects against MIA-induced inflammation and knee cartilage damage by deactivating the MAPK/NF-κB pathway in rats with osteoarthritis. *Open Life Sci*. 2020;15(1):971–980. doi:10.1515/biol-2020-0105
24. Ma C, Wu C, Jou I, et al. PKR promotes oxidative stress and apoptosis of human articular chondrocytes by causing mitochondrial dysfunction through p38 MAPK activation-PKR activation causes apoptosis in human chondrocytes. *Antioxidants*. 2019;8(9):370. doi:10.3390/antiox8090370
25. Boyle D, Hammaker D, Edgar M, et al. Differential roles of MAPK kinases MKK3 and MKK6 in osteoclastogenesis and bone loss. *PLoS One*. 2014;9(1):e84818. doi:10.1371/journal.pone.0084818
26. Rasheed Z, Akhtar N, Haqqi T. Pomegranate extract inhibits the interleukin-1β-induced activation of MKK-3, p38α-MAPK and transcription factor RUNX-2 in human osteoarthritis chondrocytes. *Arthritis Res Therapy*. 2010;12(5):R195. doi:10.1186/ar3166
27. Guma M, Hammaker D, Topolewski K, et al. Antiinflammatory functions of p38 in mouse models of rheumatoid arthritis: advantages of targeting upstream kinases MKK-3 or MKK-6. *Arthritis Rheum*. 2012;64(9):2887–2895. doi:10.1002/art.34489
28. Linda SS, David B, Deepa H, David SH, Emily AV, Gary SF. MKK3, an upstream activator of p38, contributes to formalin Phase 2 and late allodynia in mice. *Neuroscience*. 2009;162(2):462–471. doi:10.1016/j.neuroscience.2009.05.008
29. Iannone F, Bari CD, Dell'Accio F, et al. Increased expression of nerve growth factor (NGF) and high affinity NGF receptor (p140 TrkA) in human osteoarthritic chondrocytes. *Rheumatology*. 2002;41(12):1413–1418. doi:10.1093/rheumatology/41.12.1413
30. Sousa-Valente J, Calvo L, Vacca V, Simeoli R, Arévalo J, Malcangio M. Role of TrkA signalling and mast cells in the initiation of osteoarthritis pain in the monoiodoacetate model. *Osteoarthritis Cartilage*. 2018;26(1):84–94. doi:10.1016/j.joca.2017.08.006
31. Sullivan O, Kc R, Singh G, et al. Sensory Neuron-Specific Deletion of Tropomyosin Receptor Kinase A (TrkA) in Mice Abolishes Osteoarthritis (OA) Pain via NGF/TrkA Intervention of Peripheral Sensitization. *Int J Mol Sci*. 2022;23(20):12076. doi:10.3390/ijms232012076
32. Atwal J, Massie B, Miller F, Kaplan D. The TrkB-Shc site signals neuronal survival and local axon growth via MEK and P13-kinase. *Neuron*. 2000;27(2):265–277. doi:10.1016/S0896-6273(00)00035-0
33. Shi L, Yue J, You Y, et al. Dok5 is substrate of TrkB and TrkC receptors and involved in neurotrophin induced MAPK activation. *Cell Signal*. 2006;18(11):1995–2003. doi:10.1016/j.cellsig.2006.03.007
34. Chaumette T, Delay L, Barbier J, et al. c-Jun/p38MAPK/ASIC3 pathways specifically activated by nerve growth factor through TrkA are crucial for mechanical allodynia development. *Pain*. 2020;161(5):1109–1123. doi:10.1097/j.pain.0000000000001808
35. Zhang J, Yi Q, Gong M, Zhang Y, Liu D, Zhu R. Upregulation of TRPV1 in spinal dorsal root ganglion by activating NGF-TrkA pathway contributes to pelvic organ cross-sensitisation in rats with experimental autoimmune prostatitis. *Andrologia*. 2019;51(8):e13302. doi:10.1111/and.13302
36. Zixiu L, Li M, Li Z, et al. NGF signaling Exacerbates KOA peripheral hyperalgesia via the increased TRPV1-labeled synovial sensory innervation in KOA rats. *Pain Res Manag*. 2024;2024(1):1–12. doi:10.1155/2024/1552594
37. Aso K, Izumi M, Sugimura N, Okanoue Y, Ushida T, Ikeuchi M. Nociceptive phenotype alterations of dorsal root ganglia neurons innervating the subchondral bone in osteoarthritic rat knee joints. *Osteoarthritis Cartilage*. 2016;24(9):1596–1603. doi:10.1016/j.joca.2016.04.009
38. Katz B, Zaguri R, Edvardson S, et al. Nociception and pain in humans lacking a functional TRPV1 channel. *J Clin Invest*. 2023;133(3):1–17. doi:10.1172/JCI153558
39. Zhang L, Li M, Li X, et al. Characteristics of sensory innervation in synovium of rats within different knee osteoarthritis models and the correlation between synovial fibrosis and hyperalgesia. *J Adv Res*. 2022;35:141–151. doi:10.1016/j.jare.2021.06.007